ACS Combinatorial Science

Technology Note

pubs.acs.org/acscombsci

# High-Throughput Production and Structural Characterization of Libraries of Self-Assembly Lipidic Cubic Phase Materials

Connie Darmanin,*[,⊥,†] Charlotte E. Conn,[⊥,‡] Janet Newman,[†] Xavier Mulet,[‡,∥] Shane A. Seabrook,[†] Yi-Lynn Liang,[†,#] Adrian Hawley,[§] Nigel Kirby,[§] Joseph N. Varghese,[†] and Calum J. Drummond[‡]

[†]CSIRO Materials Science and Engineering, 343 Royal Parade, Parkville, Victoria 3052, Australia

[‡]CSIRO Materials Science and Engineering, Private Bag 10, Clayton South MDC, Victoria 3169, Australia

[§]Australian Synchrotron, 800 Blackburn Rd, Clayton, Victoria 3168, Australia

[∥]Drug Delivery, Disposition and Dynamics, Monash Institute of Pharmaceutical Sciences, 381 Royal Parade, Parkville Victoria 3052, Australia

[#]ARC Centre of Excellence for Coherent X-ray Science, La Trobe University, Bundoora, Victoria 3086, Australia

Supporting Information

**ABSTRACT:** A protocol is presented for the high-throughput (HT) production of lyotropic liquid crystalline phases from libraries of lipids and lipid mixtures using standard liquid dispensing robotics, implementing methods that circumvent the problems traditionally associated with handling the highly viscous cubic phase. In addition, the ability to structurally characterize lipidic phases and assess functionality for membrane proteins contained within cubic phases, in a HT manner, is demonstrated. The techniques are combined and exemplified using the application of membrane protein crystallization within lipidic cubic phases.

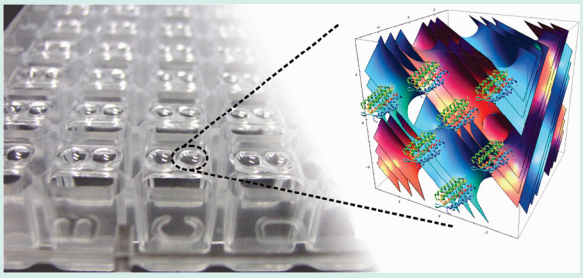

**KEYWORDS:** *membrane proteins, bicontinuous cubic phase, monoolein, high-throughput, in meso crystallization, lipid self-assembly*

The profile of lipidic mesophases has been raised over the past two decades with applications such as biosensors,[1,2] drug delivery matrixes,[3] gene therapy,[4] medical imaging,[5] and potentially within biofuel cells.[6] The lipidic cubic phase has three-dimensional periodicity and an ordered bilayer-based structure. This structure leads to amphiphilic properties, while the bicontinuous nature of the lipid bilayer and the water channel networks define many of their applications, including in meso membrane protein (MP) crystallization and drug delivery.[3,7]

Despite their potential applications, experimental difficulties that arise from the complex rheological properties of the cubic phase have hindered research efforts. Both the preparation of cubic phases and their structural characterization are notoriously time-consuming.[8] The current methods for preparing lipid mixtures (e.g., to mimic the lipid bilayer or to exert a degree of control over the nanostructure) are lengthy, and the structural assessment of the cubic phase performance requires testing under a range of chemical and physical conditions, such as incorporated additives, solvent variation, temperature and pressure, which create additional degrees of complexity.

Attempts have been made to increase the throughput of lipidic phase production,[8−10] and there has been a drive to develop commercial HT robotics specifically for in meso crystallization trials, including the Flexus Crystal IMP, Gryphon LCP (Art Robbins/Rigaku), NT8-LCP (Formulatrix), Mosquito LCP (TTP Labtech), and ProCrys Meso (Zinsser-Analytic). In addition, it has recently become possible to purchase commercial LCP kits (including the LCP screening kit (Hampton)[11]and Cubic LCP kit (Emerald bioSystems)[12]). A microfluidic device, which mixes protein directly with preformed cubic phase, has recently been used for the growth of crystals of Photosynthetic Reaction Centre from *Rhodobacter sphaeroides* and *Blastochloris viridis*.[10] While nanoliter volumes of preformed cubic phase can be dispensed (either in water or premixed with protein), difficulties persist with all of the above methods because of the requirement to premix the lipid, aqueous phase and protein solution in a coupling device.[9,10] Our method eliminates the step of premixing and allows the LCP to form directly in the crystallization plate. The LCP screen NeXtal plate (Qiagen),[13] contains lipid predispensed within each well of a crystallization plate avoiding the need for premixing. However, these plates are currently limited to a single lipid, monoolein, which may be doped with cholesterol at a single ratio (8 wt %).

To address the limitations associated with the commercial products, namely, their high specificity, expense, and the necessity to manually premix solutions, a novel HT method for cubic phase formation using standard liquid dispensing robotics was developed. Dry lipid is initially dissolved in a carrier solvent

**Received:** October 17, 2011
**Revised:** February 1, 2012
**Published:** March 19, 2012

(typically ethanol), as described by Rummel et al., to reduce the viscosity and allow for easier dispensing.[14] The novelty of our approach is that the lipid solution may then be dispensed accurately from any positive displacement liquid dispensing robot to a standard Society for Biomolecular Sciences (SBS) crystallization plate (96 or higher density, Figure 1a). Following

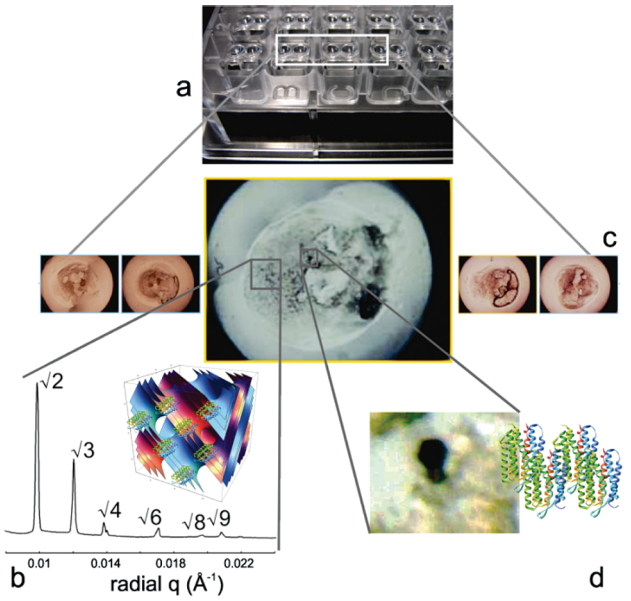


**Figure 1.** Schematic of the multiple techniques compatible with cubic phase using the protocol described herein. (a) 96-well SBS plate, (b) a schematic of Bacteriorhodopsin (bR) incorporated within the MO diamond ($Q_{II}^{D}$) cubic phase; a typical 1-D diffraction pattern of intensity vs scattering vector q for this system. (c) Images from 5 separate wells of a shower of bR crystals grown within the MO $Q_{II}^{D}$ cubic phase using this protocol. bR crystals ranged, in the largest dimension, from 10 to 20 $\mu$m. Images taken using the Minstrel HT imager (Rigaku) and (d) an enlarged image of a single crystal of bR taken using an Olympus SZX12 Stereomicroscope.

evaporation of the solvent, the cubic phase will form spontaneously in situ via the addition of an aqueous phase. In this way production of the cubic phase may be performed in a high-throughput manner entirely using robotics, avoiding the need to use a coupled syringe device or to handle viscous LCP. The strategy was found to be compatible with a range of lipids including monoolein (MO),[15] phytantriol,[16] monopalmitolein, monovaccenin,[17] and cholesterol, and therefore applicable to the HT production of combinatorial libraries for complex lipid mixtures.

**Validation of the Method.** Formation of the cubic phase via the above method was confirmed using small-angle X-ray scattering (SAXS). The crystallization plates can be mounted directly in a synchrotron SAXS beamline, which allows in situ characterization of the mesophase structure. Diffraction characteristic of a self-assembled mesophase can be detected at least down to 20 $\mu$g of lipid (hydrated with 13.6 nl water) for both MO[15] and phytantriol.[16] This is comparable to the sample volume used by the Flexus Crystal IMP robot.[18] However, at sample masses below 100 $\mu$g of lipid, we observed inconsistent phase behavior, described in detail in the Experimental Procedures (Optimization of Sample Mass). Therefore, for SAXS analysis, sample size was maintained >100 $\mu$g of lipid. To ensure reproducibility, the structures of 10 or more replicates of 8 different lipids (or lipid mixtures) were characterized using the SAXS beamline at the Australian Synchrotron. The samples contained 60 wt % lipid (210 $\mu$g), 40 wt % water (140 $\mu$g), and consistently formed a diamond cubic phase ($Q_{II}^{D}$); a typical 1-D SAXS pattern of intensity vs q for MO is shown in Figure 1b. A minimum of seven diffraction peaks were obtained for each cubic phase using 1s exposures. For MO, the average lattice parameter was 99.9 Å with a standard deviation of 0.8 Å (for 36 samples). The standard deviation is low for such a large number of samples; a similar standard deviation was observed in the lattice parameter of only four samples produced using conventional mixing methods. A more complete comparison of the robotic setup versus conventional sample preparation techniques both using coupled syringes, and in vials, is provided in the Supporting Information, Figure S1−S3 and Table S2. Reproducibility in phase behavior was confirmed for all samples tested, although an increase in the standard deviation was noted for high cholesterol concentrations (Supporting Information, Table S1). Homogeneity of the cubic phase within each well was confirmed, with no variation being observed over the entire surface of the well (data not shown). Note that although formation of a homogeneous cubic phase was found to be fast (<1 h post-hydration) Wallace et al.[9] have recently suggested that protein reconstitution within the cubic phase may require longer incubation times.

Following HT production of the cubic phase we now demonstrate two fundamental characterization techniques, SAXS characterization and ligand binding studies, which may be carried out in a HT manner in situ within the 96-well plate.

**High-Throughput SAXS Structural Characterization.** The ability to mount a crystallization plate directly in a synchrotron SAXS beamline provides a powerful tool for collecting HT in situ SAXS data, for example, determining the nanostructure of libraries of self-assembling amphiphilic materials. Up to two plates are contained within a temperature-controlled plate holder. Automated image acquisition by raster scanning through 192 wells (96 duplicate conditions) can be completed in 35 min. The subsequently large data sets can be analyzed in a HT manner using the IDL-based AXcess software package.[19] Importantly, this protocol allows samples with a mass of 100 $\mu$g to be characterized, a reduction of 2 orders of magnitude compared to traditional capillary or plate cells (typically 20 mg).

**GPCR Ligand-Binding Assays.** Traditionally, ligand-binding assays on MPs contained within a cubic phase required manual mixing of dry lipid with the protein solution using coupled Hamilton syringes;[20] however, applying a slightly modified HT protocol allows rapid assessment of protein functionality for samples which have been robotically dispensed into 96-well filtration plates. Functionality was determined via radio-labeled ligand-binding assays, which are routinely used for GPCRs to assess the amount of ligand bound to a particular receptor and indicate whether the protein has retained a functional conformation. Figure 2a and b presents the typical saturation binding curves for Dopamine 2 Long receptor (D2L) and Histamine H1 receptor (H1R) both reconstituted in MO, and in detergent solubilized form. Negative controls confirm nonspecific binding of the ligands to the lipid (MO) in the assay (Figure 2c and Supporting Information, Figure S6b). Additional controls and saturation curves of total vs nonspecific binding for both D2L and H1R can be found in the Supporting Information, Figures S5−S8. The significant increase in binding activity for both receptors, when reconstituted into MO cubic phase, as compared to the detergent solubilized form (Figure


dx.doi.org/10.1021/co2001718 | ACS Comb. Sci. 2012, 14, 247−252

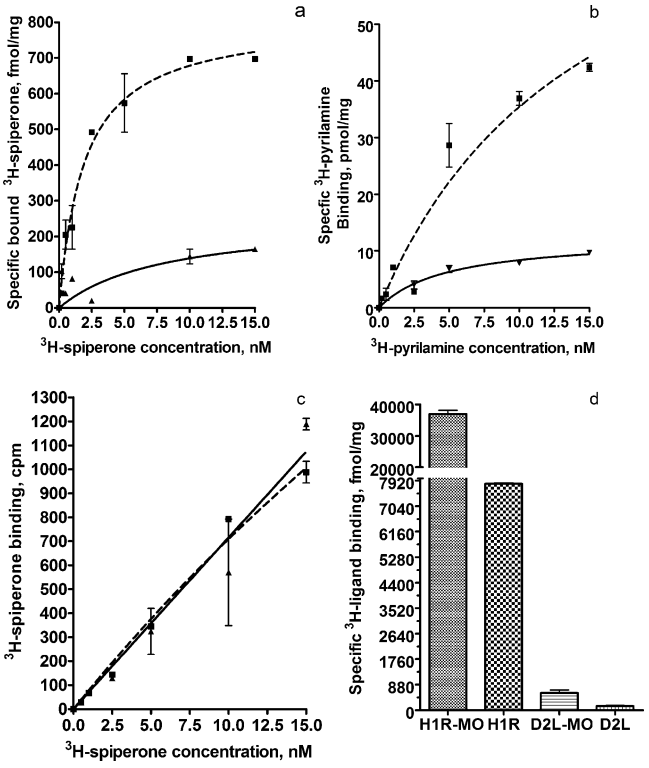


**Figure 2.** Typical radio-ligand binding assays for H1R and D2L preparations. Preparations represent the H1R and D2L receptors after purification and reconstitution into the monoolein (MO) cubic phase. (a) Saturation radio-ligand binding experiments using detergent solubilized D2L (solid line) and reconstituted D2L −MO (dashed line), that in each set yielded a single high affinity binding site for $^3$H-Spiperone, $K_d$ = 1.9 nM and 8.0 nM, respectively. (b) Saturation radio-ligand binding experiments using detergent solubilized H1R (solid line) and reconstituted H1R −MO (dashed line), that in each set yielded a single high affinity binding site for $^3$H-pyrilamine, $K_d$ = 4.8 nM and 14.8 nM, respectively. (c) A negative control saturation binding curve for $^3$H-spiperone showing nonspecific binding to MO. Total binding (■, solid line) and nonspecific binding (▲, dashed line) for $^3$H-spiperone binding to MO with no receptor is shown. (d) Specific ligand-binding of two purified receptors: H1R and D2L, and these receptors reconstituted into MO: H1R-MO and D2L-MO, respectively. This result is based on 10 nM of radio-ligand being added to the assay.

2d) is indicative of successful receptor reconstitution into the lipid bilayer.

**In Meso Crystallization.** The HT production and characterization techniques were demonstrated by completing in meso crystallization of the MP, bacteriorhodopsin (bR), using the lipidic cubic phase as a matrix for crystal growth. Advances in using this promising technique have been hindered by difficulties in handling the cubic phase; only 79 structures of 17 unique MPs have been solved to date using in meso crystallization.[21]

On the basis of published crystallization conditions[22−24] the growth of bR MP crystals in monoolein and monopalmitolein cubic phase, produced using the HT method in SD-2 crystallization plates, was successful. An imaging robot (Minstrel HT Rigaku) at the CSIRO C$^3$ facility was used for incubation and visualization of the crystallization plates. A typical image of bR crystals obtained using this protocol is shown in Figure 1c with an enlarged image of a single bR crystal shown in Figure 1d. Using this protocol, crystal growth occurred without a lengthy preincubation of the protein within the cubic phase prior to addition of crystallant. However, it has been recently suggested that much longer incubation times may be required for effective protein reconstitution within the cubic phase,[9] depending on the protein and detergent environment. We therefore suggest that the preincubation time is optimized for individual experiments.

The described HT protocols were used to characterize both the cubic phase nanostructure and the incorporated MP. SAXS characterization can monitor the changes in the cubic phase over the period of crystal growth, which has potential to improve the fundamental understanding of the evolution of phase behavior under in meso crystallization conditions. While it is important to understand the effect of the crystallant components on the structure of the cubic mesophase, the variable physiochemical space for crystallization is so large that it would be unreasonable to explore this using traditional experimental methods. Recently, we and others[25,26] have applied HT methods to study the cubic phase under crystallization conditions; a typical data set (Supporting Information, Figure S4) displays the phase adopted by the lipid MO (40% w/v water) under the influence of the components from the PACT crystallization screen.[27]

To summarize, an easy to implement and reliable method for handling the bicontinuous cubic phase using standard robotics has been developed. The method is applicable to any combination of lipids, additives, and solvents and is accurate for sample masses down to 100 μg. The protocol is compatible with a variety of techniques suitable for characterizing the structure of the lipid mesophase, and the properties of biologics. The method can facilitate the development of commercial applications for cubic phase technology in a number of areas including pharmaceutical (drug discovery, drug delivery, gene therapy and medical imaging), materials science (biosensors, emulsifiers, biofuel cells, detergent industries), biology (long-term storage of fragile proteins, determining transport mechanisms for MPs, crystallization) and chemistry/physics (fundamental surfactant and lipid phase behavior studies), which are currently restricted by difficulties in handling this highly viscous material. With over 80 surfactants/lipids having been identified as forming cubic phases in aqueous solution,[28] the new protocol also creates the opportunity to readily investigate lipid diversity, rapidly construct detailed phase diagrams, and investigate in meso crystallization of MPs, which relies on diverse physicochemical studies.

## ■ EXPERIMENTAL PROCEDURES

**Materials.** The purple membrane form of Bacteriorhodopsin expressed in *Halobacterium Salinarum* was purchased from Sigma-Aldrich (B0184). Buffer components were purchased from Sigma Aldrich unless otherwise stated. SD-2 96-well crystallization plates (IDEX corp, CA) were purchased from IDEX. The PACT[27] crystallization screen was either purchased through Qiagen (The PACT suite, catalogue number 130718) or made within the CSIRO C$^3$ facility using stocks created in-house. The ligand-binding filtration plate was purchased from Millipore, MultiScreen HTS 96-Well Filter Plates (MSHVN4B10).

1-Monoolein and cholesterol were purchased from Sigma-Aldrich. Monovaccenin and monopalmitolein were purchased from Nu-Chek Prep. 3,7,11,15-Tetramethyl-1,2,3-hexadecane-


dx.doi.org/10.1021/co2001718 | ACS Comb. Sci. 2012, 14, 247−252

triol (phytantriol) (96%) was provided by DSM Nutritional Products, Germany.

**Methods.** *Lipid Dispensation into Plates.* All lipids were made up to 200 mg/mL in ethanol. The lipid solution was dispensed into SD-2 96-well plates using the Mosquito robot, (TTP Labtech, Melbourn, U.K.) located within the CSIRO $C^3$ facility. For 200 mg/mL lipid solution, 1.05 $\mu$L lipid (0.21 mg) was deposited in each subwell of a 96-well plate. The plates were dried in a vacuum oven at 40 °C and 0.2 MPa overnight and allowed to thoroughly dry in a fume hood for a further day before aqueous phase (water or protein solution) was added. The temperature of the oven may be adjusted as desired based on the decomposition properties of individual lipids. The lipid solution dries to form a thin film covering the bottom of the well. At this point, we found that plates could be stored at either −20 °C or at room temperature, depending on the stability of the lipid, for months, without adversely affecting the phase behavior.

Generally, 0.14 $\mu$L of aqueous solution (buffer or protein solution) was then dispensed onto the film of dry lipid to give the ratio 60:40 (w/v) of lipid/aqueous solution. The cubic phase forms spontaneously upon addition of the aqueous solution. Because of the thin film nature of the dried lipid, equilibration times are fast; we observed a homogeneous hydrated cubic phase via SAXS within 1 h of hydration. Note, however, that as recently described in Wallace et al, longer preincubation times for the cubic phase may be required for effective protein reconstitution and crystal growth.[9] 20−50 $\mu$L of crystallant or water was also added to each reservoir well to ensure that the cubic phase did not dry out during data collection.

*Optimization of Sample Mass.* The lipid mass was minimized while retaining adequate volume to allow for visualization of the cubic phase mixture using the available crystallization imaging system (Minstrel HT, Rigaku California), and to provide an adequate signal-to-noise ratio for SAXS experiments. Various volumes of lipid solution corresponding to lipid quantities of 210 $\mu$g to 2 $\mu$g of either of two different lipids (monoolein or phytantriol) were deposited within a 96-well plate. Water was added in the ratio 60:40 (w/v), lipid/water. It was found that clear diffraction patterns (with at least four orders of Bragg peaks) were obtained down to a sample mass of 20 $\mu$g of lipid. For MO, a $Q_{II}^D$ phase (lattice parameter 103.2−105.9 Å) was retained for lipid masses ≥50 $\mu$g, with a gyroid cubic phase observed for samples <20 $\mu$g. For phytantriol, a $Q_{II}^D$ phase was observed for sample masses down to 10 $\mu$g, with lattice parameters in the range 67.9−68.8 Å, consistent with the published phase behavior for phytantriol.[16] At extremely small sample masses ≤5 $\mu$g a phase change to an inverse hexagonal mesophase was observed. We suggest that the different phases observed at extremely low water content may reflect both errors in dispensing small volumes of water by the Mosquito robot, and increased drying effect associated with small sample size. The gyroid cubic phase (for MO) and $H_{II}$ phase (for Phytantriol) are typically observed at lower water contents than their respective $Q_{II}^D$ phases. While the $H_{II}$ phase is observed in the published phase diagram for phytantriol at temperatures >43 °C, recent research has suggested than inherent impurities in commercial grade phytantriol can significantly affect the phase boundary temperatures.[29]

*Purification of Bacteriorhodopsin.* The purple membrane-form of bR expressed in *H. Salinarum* was purified using established protocols.[23] Briefly, the bR was extracted from the membrane using $NaH_2PO_4$ buffer (pH 6.9) and *n*-octyl-$\beta$-D-glucoside (nOG) and purified using gel filtration in 25 mM $NaH_2PO_4$ pH 5.5 and 1.2% nOG buffer. The purified bR was concentrated to 20 mg/mL for crystallization trials (using a Millipore spin concentrator with a 10K MW cutoff).

*Crystallization of Bacteriorhodopsin (bR).* Crystallization trials using bR were set up using the protocol above, a modification of the method outlined in Nollert and Landau et al.[22,23] was used. Briefly, 100 $\mu$g of either monoolein (MO) or monopalmitolein (MP) was deposited into the subwells of crystallization plates using the protocol described above. 0.067 $\mu$L of bR was deposited on top of the dry lipid immediately followed by 0.067 $\mu$L of crystallant. 50 $\mu$L of crystallant was added to the reservoir. A series of 24 wells were set up in duplicate for each lipid. The MO wells contained 9 mg/mL bR, and 27% PEG 6000 in 100 mM $Na_2HPO_4/KH_2PO_4$, pH 5.6 as the crystallant, and the MP wells contained 20 mg/mL bR and 1 M $Na_2HPO_4$ /$KH_2PO_4$ pH 5.5, 2.5% 2-methyl-2,4-pentanediol (MPD) as the crystallant. After dispensing the protein solution and crystallants, the plates were sealed using the Crystal Clear Sealing Film (HR3-609 Hampton Research, CA) and stored at 20 °C in the dark. Plates were imaged with the Minstrel HT imager (Minstrel HT, Rigaku California) according to the standard $C^3$ schedule (4 inspections in the first week, 2 in the second week, and subsequently weekly for a total of 14 inspections). Images were viewed with the CrystalTrak (Rigaku) application or plates were examined using an Olympus SZX12 stereomicroscope.

*Small Angle X-ray Scattering (SAXS) Characterization.* The structures of the mesophases formed in situ within a 96-well plate using the protocol described above were determined using SAXS, which provides information on the particular mesophase adopted, and on the lattice parameter, or unit cell size. Data were obtained at the SAXS/WAXS beamline of the Australian Synchrotron; a typical experiment used a beam of wavelength $\lambda$ = 1.0332 Å (12.000 ± 0.002 keV) with dimensions 250 $\mu$m × 120 $\mu$m, a sample to detector distance of 1100 mm, and a typical flux of 5 × $10^{12}$ photons/s. 2-D diffraction images were recorded on a Pilatus 1-M detector.

A custom-designed plate-holder allowed any crystallization plate with a standard SBS footprint (85 × 127 mm, 96, or 384 well) to be mounted directly in the beam for in situ SAXS analysis. The temperature-controlled plate-holder consists of a stainless steel box with temperature control provided via fan-forced air-temperature controlled airflow. The air is forced over a Peltier controlled heat exchanger, backed by a water cooled/heated plate running from a water bath. Temperature is controlled at the sample position itself because of significant airflow, that is, there is very little reliance on conduction inside the sample volume. Data were acquired in an automated fashion using a preloaded set of positions based on the layout of the plate. Using a typical exposure time of 1 s, 192 samples (96 wells run in duplicate) were screened in 35 min. Although 20−50 $\mu$L of crystallant or water was added to the reservoir subwell of the SD-2 plate, by gently rotating the plate into the holder the contents of the reservoir did not move during loading of the plates in to the holder.

*SAXS Data Analysis.* All images were analyzed using AXcess, a SAXS analysis program written by Andrew Heron.[19] AXcess allows for batch processing and analysis of the large X-ray data sets produced by high-throughput synchrotron experiments. It can integrate thousands of images sequentially, producing a


dx.doi.org/10.1021/co2001718 | ACS Comb. Sci. 2012, 14, 247−252

"stacked" plot of 1-D images with time. Providing the underlying mesophase symmetry remains constant (as is the case for many groups of wells within each plate), the program can then fit pre-specified peaks within each 1-D pattern, exporting an ascii file of the *d*-spacing as a function of image number.

*Protein Expression and Purification of Receptors.* Expression and purification of human Histamine H1 Receptor (H1R) and human Dopamine 2 Long Receptor (D2L) are described in detail in the Supporting Information, Methods section.

Functional studies on purified H1R and D2L were carried out using [$^3$H] radio-labeled antagonist binding assays as outlined below. The purity of the proteins were checked on an SDS-PAGE and via Western blots (unpublished data). The concentration of H1R and D2L receptor were determined according to Bradford's method using bovine serum albumin as a standard.[30]

*Ligand Binding Assay.* Radioligand binding assays and data analyses were performed as described in Ratnala et. al[31] with modifications as described below. Millipore MultiScreen HTS 96-Well filter plates were used for the [$^3$H] radio-label binding assays. All assays were carried out in triplicate wells on the same plate using the same batch of protein. The lipids were made up to 200 mg/mL in ethanol and 1 mg of lipid was deposited into each well using the Mosquito robot. The plate was incubated at 40 °C in a vacuum oven (0.2 MPa) to allow the solvent to evaporate. A minimum of 5 $\mu$g of purified receptor was dispensed on top of the dried lipid film in each well, and the volume of protein added was at a 60:40 ratio of lipid to protein. This was immediately followed by deposition of TMN buffer (50 mM Tris, 10 mM $MgCl_2$, 100 mM NaCl, pH 7.6). Nonspecific radio-ligand binding was determined by addition of unlabeled ligand, 160 $\mu$M tripelennamine for H1R or 2.1 $\mu$M spiperone for D2L, to the reaction mix in alternative wells. The total volume of the assay was 50 $\mu$L, and the volume of TMN added per assay was determined accordingly.

10 nM [$^3$H]-pyrilamine (Perkin-Elmer) or 10 nM [$^3$H]-Spiperone was added last to the reaction mix to give a final volume of 50 $\mu$L. The concentration of the radio-labeled ligand was determined based on the saturation binding curves. The final MP concentration in the assay was determined such that less than 10% of total radio-ligand was receptor-bound based on the saturation binding assay curves. The assays were incubated, with shaking, in a 27 °C water bath for 30 min. The assay was terminated by rapid filtration over a 96 well filtration plate system (Millipore) for the lipid assays. For the detergent solubilized assay, an equal volume of ice cold 30% PEG400 was added to the samples and incubated on ice for a further 15 min to precipitate the receptor before filtration over the 96 well filtration plate system (Millipore). The excess unbound ligand in the assay was removed by thoroughly washing the samples with 10 × 200 $\mu$L of TMN buffer and filtering it through the wells. The plate was dried overnight.

Ultima Gold (Perkin-Elmer) liquid scintillant (50 $\mu$L) was added to each well and beta radiation was detected in a Wallac MicroBeta TriLux 1450LSC and Luminescence Counter (Perkin-Elmer). The plates were sealed with adhesive clear film and each channel was counted for 20 s. The specific binding was calculated based on the counts per million (cpm). Several controls were set up, including negative controls (without receptor, with receptor, and in the presence of saturated amounts of cold ligand and receptor plus a nonspecific $^3$H-ligand) and a positive control consisting of detergent solubilized protein without lipid. For the saturation binding curves the concentration of radio-labeled ligand in the reaction was varied from 0 to 15 nM. Binding data were evaluated by a nonlinear, least-squares curve-fitting procedure using GRAPHPAD PRISM4 (GRAPHPAD Software, Inc., San Diego, CA). The ligand affinities were calculated according to Swillens[32] by using a global fitting procedure to determine total and nonspecific binding at the same time. Nonspecific binding was determined by saturation binding experiments, which estimated nonspecific binding under total binding conditions. Note the choice of ligand in the purification buffer was selected based on their low binding affinity to the receptors in respect to the radio-ligands. Therefore, the radio-ligands (which have a higher affinity for the receptors) will compete for binding to the receptors providing a reliable assay result.

## ■ ASSOCIATED CONTENT

### Supporting Information

Methods on GPCR expression and purification; tabulated data on the average lattice parameters of monoolein (MO), monopalmitolein (MP), monovaccenin (MV) and cholesterol (chol) mixtures; comparison of the phase behavior of MO 40% (w/w) $H_2O$ samples produced via conventional, robotic, and syringe-based preparation methods; representative 1-D diffraction plots of intensity vs q for samples produced via conventional, robotic, and syringe-based preparation methods; a schematic showing the distribution of phases across a two subwell crystallization plate 1 day after addition of PACT screen to monoolein (40% w/v water); total and nonspecific saturation binding curves for D2L and H1R with negative control data. This material is available free of charge via the Internet at http://pubs.acs.org.

## ■ AUTHOR INFORMATION

### Corresponding Author

*Phone: +613 9662 7136. Fax: +61 3 9662 7101. E-mail: connie.darmanin@csiro.au.

### Author Contributions

⊥These authors contributed equally to the work.

### Funding

Part of this research was undertaken on the SAXS/WAXS beamline at the Australian Synchrotron, Victoria, Australia the CSIRO C$^3$ facility and CSIRO fermentation facility, Parkville, Victoria, Australia. The authors thank the CSIRO Preventative Health Flagship and Capability Development Fund for funding and the ARC Centre of Excellence for Coherent X-ray Science. C.J.D. was the recipient of an Australian Research Council Federation Fellowship. C.E.C. was the recipient of a CSIRO OCE Postdoctoral Fellowship.

### Notes

The authors declare no competing financial interest.

## ■ ABBREVIATIONS

C3: The CSIRO Collaborative Crystallization Centre (Melbourne, Australia); bR: bacteriorhodopsin; D2L: Dopamine 2 long receptor; H1R: Histamine H1 receptor; HT: high-throughput; LCP: lipidic cubic phase; MP: membrane protein; MO: monoolein; Phy: phytantriol; SAXS: Small Angle X-ray Scattering; SBS: Society for Biomolecular Sciences

## REFERENCES


(1) Nazaruk, E.; Bilewicz, R.; Lindblom, G.; Lindholm-Sethson, B. Cubic phases in biosensing systems. *Anal. Bioanal. Chem.* **2008**, *391* (5), 1569−1578.

(2) Angelova, A.; Ollivon, M.; Campitelli, A.; Bourgaux, C. Lipid cubic phases as stable nanochannel network structures for protein biochip development: X-ray diffraction study. *Langmuir* **2003**, *19* (17), 6928−6935.

(3) Boyd, B. J. Past and future evolution in colloidal drug delivery systems. *Expert Opin. Drug Delivery* **2008**, *5* (1), 69−85.

(4) Chonn, A.; Semple, S. C.; Cullis, P. R. Association of Blood Proteins with Large Unilamellar Liposomes Invivo - Relation to Circulation Lifetimes. *J. Biol. Chem.* **1992**, *267* (26), 18759−18765.

(5) Moghaddam, M. J.; de Campo, L.; Waddington, L. J.; Weerawardena, A.; Kirby, N.; Drummond, C. J. Chelating oleyl-EDTA amphiphiles: self-assembly, colloidal particles, complexation with paramagnetic metal ions and promise as magnetic resonance imaging contrast agents. *Soft Matter* **2011**, *7* (22), 10994−11005.

(6) Nazaruk, E.; Smolinski, S.; Swatko-Ossor, M.; Ginalska, G.; Fiedurek, J.; Rogalski, J.; Bilewicz, R. Enzymatic biofuel cell based on electrodes modified with lipid liquid-crystalline cubic phases. *J Power Sources* **2008**, *183* (2), 533−538.

(7) Caffrey, M. Crystallizing Membrane Proteins for Structure Determination: Use of Lipidic Mesophases. *Annu. Rev. Biophys.* **2009**, *38*, 29−51.

(8) Imberg, A.; Engstrom, S. An increased throughput method for determination of phase diagrams - method development and validation. *Colloids Surf., A* **2003**, *221* (1−3), 109−117.

(9) Wallace, E.; Dranow, D.; Laible, P. D.; Christensen, J.; Nollert, P., Monoolein Lipid Phases as Incorporation and Enrichment Materials for Membrane Protein Crystallization. *Plos One* **2011**, *6* (8).

(10) Li, L.; Fu, Q.; Kors, C. A.; Stewart, L.; Nollert, P.; Laible, P. D.; Ismagilov, R. F. A plug-based microfluidic system for dispensing lipidic cubic phase (LCP) material validated by crystallizing membrane proteins in lipidic mesophases. *Microfluid. Nanofluid.* **2010**, *8* (6), 789−798.

(11) Hampton LCP Lipidic Cubic Phase screening kit. http://hamptonresearch.com/product_detail.aspx?cid=10&sid=182&pid=600.

(12) Emerald; Biosystems Cubic LCP Kit.

(13) Qiagen, *NexTal Cubic Phase Handbook*; Qiagen: Hilden, Germany, 2009; p 7.

(14) Rummel, G.; Hardmeyer, A.; Widmer, C.; Chiu, M. L.; Nollert, P.; Locher, K. P.; Pedruzzi, I.; Landau, E. M.; Rosenbusch, J. P. Lipidic cubic phases: New matrices for the three-dimensional crystallization of membrane proteins. *J Struct. Biol.* **1998**, *121* (2), 82−91.

(15) Briggs, J.; Chung, H.; Caffrey, M. The temperature-composition phase diagram and mesophase structure characterization of the monoolein/water system. *J. Phys. II* **1996**, *6* (5), 723−751.

(16) Barauskas, J.; Landh, T. Phase behavior of the phytantriol/water system. *Langmuir* **2003**, *19* (23), 9562−9565.

(17) Qiu, H.; Caffrey, M. Lyotropic and thermotropic phase behavior of hydrated monoacylglycerols: Structure characterization of monovaccenin. *Biophys. J.* **1998**, *74* (2), A374−A374.

(18) Cherezov, V.; Peddi, A.; Muthusubramaniam, L.; Zheng, Y. F.; Caffrey, M. A robotic system for crystallizing membrane and soluble proteins in lipidic mesophases. *Acta Crystallogr, Sect. D* **2004**, *60*, 1795−1807.

(19) Seddon, J. M.; Squires, A. M.; Conn, C. E.; Ces, O.; Heron, A. J.; Mulet, X.; Shearman, G. C.; Templer, R. H. Pressure-jump X-ray studies of liquid crystal transitions in lipids. *Philos. Trans. R. Soc., A* **2006**, *364* (1847), 2635−2655.

(20) Cheng, A.; Hummel, B.; Qiu, H.; Caffrey, M. A simple mechanical mixer for small viscous lipid-containing samples. *Chem. Phys. Lipids* **1998**, *95* (1), 11−21.

(21) Cherezov, V. Lipidic cubic phase technologies for membrane protein structural studies. *Curr. Opin. Struct. Biol.* **2011**, *21* (4), 559−566.

(22) Landau, E. M.; Rosenbusch, J. P. Lipidic cubic phases: A novel concept for the crystallization of membrane proteins. *Proc. Natl. Acad. Sci. U.S.A.* **1996**, *93* (25), 14532−14535.

(23) Nollert, P. Lipidic cubic phases as matrices for membrane protein crystallization. *Methods* **2004**, *34* (3), 348−353.

(24) Nollert, P.; Royant, A.; Pebay-Peyroula, E.; Landau, E. M. Detergent-free membrane protein crystallization. *Febs Lett.* **1999**, *457* (2), 205−208.

(25) Joseph, J.; Lui, W.; Kunken, J.; Weiss, M.; Tsuruta, H.; Cherezov, V. Characterization of lipidic matrices for membrane protein crystallization by high-throughput small angle X-ray scattering. *Methods* **2011**, *55* (4), 342−349.

(26) Conn, C. E.; Darmanin, C.; Mulet, X.; Kirby, N.; Drummond, C. J. High-throughput in situ analysis of the structural evolution of the monoolein cubic phase under crystallogenesis conditions. *Soft Matter* **2012**, *8* (7), 2310−2321.

(27) Newman, J.; Egan, D.; Walter, T. S.; Meged, R.; Berry, I.; Ben Jelloul, M.; Sussman, J. L.; Stuart, D. I.; Perrakis, A. Towards rationalization of crystallization screening for small- to medium-sized academic laboratories: the PACT/JCSG plus strategy. *Acta Crystallogr., Sect. D* **2005**, *61*, 1426−1431.

(28) Fong, C.; Le, T.; Drummond, C. J. Lyotropic liquid crystal engineering-ordered nanostructured small molecule amphiphile self-assembly materials by design. *Chem. Soc. Rev.* **2012**, *41* (3), 1297−322.

(29) Dong, Y. D.; Dong, A. W.; Larson, I.; Rappolt, M.; Amenitsch, H.; Hanley, T.; Boyd, B. J. Impurities in commercial phytantriol significantly alter its lyotropic liquid-crystalline phase behavior. *Langmuir* **2008**, *24* (13), 6998−7003.

(30) Bradford, M. M. Rapid and Sensitive Method for Quantitation of Microgram Quantities of Protein Utilizing Principle of Protein-Dye Binding. *Anal. Biochem.* **1976**, *72* (1−2), 248−254.

(31) Ratnala, V. R. P.; Swarts, H. G. P.; VanOostrum, J.; Leurs, R.; DeGroot, H. J. M.; Bakker, R. A.; DeGrip, W. J. Large-scale overproduction, functional purification and ligand affinities of the His-tagged human histamine H1 receptor. *Eur. J. Biochem.* **2004**, *271* (13), 2636−2646.

(32) Swillens, S. Interpretation of Binding Curves Obtained with High Receptor Concentrations - Practical Aid for Computer-Analysis. *Mol. Pharmacol.* **1995**, *47* (6), 1197−1203.